Heliyon 9 (2023) e18524

Contents lists available at ScienceDirect

Heliyon

journal homepage: www.cell.com/heliyon

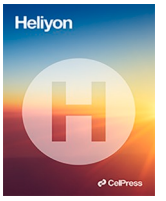

Structural and optical behaviours of methyl acrylate-vinyl acetate composite thin films synthesized under dynamic low-pressure plasma

Md Saddam Sheikh [a], Md Juel Sarder [a], A.H. Bhuiyan [a,b], Mohammad Jellur Rahman [a,*]

[a] Department of Physics, Bangladesh University of Engineering and Technology, Dhaka-1000, Bangladesh
[b] University of Information Technology and Sciences, Baridhara, Dhaka-1212, Bangladesh

ARTICLE INFO

Keywords:
Methyl acrylate
Vinyl acetate
Dynamic low-pressure plasma
Composite thin films
Optical band gap
UV–Vis spectroscopy

ABSTRACT

Low-pressure (33.33 Pa) plasma polymerized methyl acrylate and vinyl acetate composite thin films with various monomer compositions were deposited onto glass substrates. Under the same plasma conditions, the homopolymer thin films were also prepared. The thickness of the composite films was observed to vary between 117 and 213 nm depending on the monomer ratio. The composite films exhibit a smooth, pinhole-free, and immaculate surface morphology, surpassing that of the homopolymers. The energy dispersive x-ray study shows that the films contain mainly carbon and oxygen with 26.09–37.20 at% and 35.03 – 40.10 at%, respectively. The composite films contain more carbon contents which enhance the film stability. The appearance of some broad absorption bands in the Fourier transform infrared spectroscopy indicates structural changes in the PP films caused by the restructuring or dilapidation of monomer molecules while forming the polymer. The UV–visible spectra analysis reveal that the composite films exhibited a tunable optical band gap by adjusting the monomer ratio. The decrease of methyl acrylate monomer reduces the direct and indirect optical band-gap values of composite films from 3.15 to 3.00 eV and 2.35 to 1.74 eV, respectively. While Urbach energy values increases from 0.33 eV to 0.90 eV. All the films showed good transmittance properties (86 – 96%) in the visible range wavelength (550 – 800 nm). Other optical parameters are also found better in composite films which indicates the aptness of the composite films in various optoelectronic or electronic applications.

1. Introduction

Organic thin film coatings have gained popularity due to their alluring properties and wide range of applications in nonlinear optics, surface hardening tools, sacrificial layers, numerous spaceship components, molecular as well as microelectronic devices [1–3]. Polymeric materials obtained from environmentally friendly sources are more crucial for obtaining biocompatible and biodegradable, and safe electrical, electronic, or optoelectronic devices to cope up with electronic garbages [4,5]. In addition, organic thin film coatings have found potential applications in microsensor technologies [6] including light-emitting diodes, organic solar cells,

* Corresponding author.
E-mail address: mjrahman@phy.buet.ac.bd (M.J. Rahman).

https://doi.org/10.1016/j.heliyon.2023.e18524
Received 18 May 2023; Received in revised form 18 July 2023; Accepted 20 July 2023
Available online 20 July 2023

photo-detectors, photodiodes, and surface modification for biomedical engineering [7–9]. However, the composition of two or more monomers may create better material systems with novel features for specific applications and has been significantly developed in several sectors to satisfy new market applications at the lowest possible price [10]. These market demands have encouraged the creation of new material mixtures, alloys, and composites. There are numerous advantages of creating composite thin films with modified electrical, mechanical, and optical properties [11] and may be important for metal protection, design of complex materials to realize biocompatible applications [12].

The plasma polymerization technique would be chosen from versatile deposition mechanisms to obtain such composite thin films, because this method does not require any solvent or initiator during the polymer formation, produces no liquid organic waste, and has no effect on the environment. With these advantages including ease of synthesis, low-cost, and lack of thermal heating the dynamic low-pressure capacitively coupled plasma polymerization approach has been used for depositing composite polymer film [13,14]. Moreover, the presence of two organic monomers increases polymerization rates and expands the range of polymer characteristics [15].

A lot of research on thin films has been done investigating different properties of organic plasma polymerized (PP) thin films, however, the research on the effect of mixing two or more organic monomers for preparing composite polymer thin films is scanty in the literature. Only a few works on bilayer and composite films reported in the literature but the deposition techniques are different from ours [6,10,16,17]. Polythiophene/poly (vinyl acetate) composite films were prepared using oxidative polymerization technique and reported that due to the nucleation effect of poly (vinyl acetate), the amount of agglomeration increased in the composite film, which has promising potential in optoelectronic applications [10]. In other studies, Islam et al. synthesized composite polymer of vinyl acetate and methyl methacrylate by suspension polymerization technique and found that the surface of the composite polymer is rougher but thermally more stable compared to those of homopolymer [16]. Kamal and Bhuiyan [18] used low-pressure glow discharge plasma system to deposit bilayer thin films of pyrrole and N,N, 3,5-tetramethylaniline. The bilayer films are observed to have different structures as well as larger energy band gaps compared to the individual monolayer films which were increased owing to the oxidation of the film at the inter-layer interface during the subsequent deposition. In another research work the block composite of methyl acrylate (MA) and vinyl acetate (VA) was prepared using photo-induced controlled radical polymerization [19] and reported that the propagation rate constant of VA was less compared to that of MA, which caused the lower polymerization rate when a higher amount of VA was used in the composition. A recent research work on pyrrole and aniline composite reported that thickness, surface morphology, and resistance of the composite films depend significantly on the variation of the individual monomer concentrations mainly because of the rapid incorporation or rearrangement of the monomers [20].

In this study, MA and VA have been chosen to produce the composite films, because VA has been widely studied owing to its biocompatibility, excellent optical properties, and few foreign-body reaction properties [16,21,22]. Besides, having a particular electron donating group connected to the vinyl group, VA is considered a less-activated monomer [19]. The MA is chosen as the second monomer because of its high optical transmittance and different applications in coatings, varnishes, adhesives, food packaging, and cosmetics [23]. By incorporating MA and VA monomers into the PP polymer chain, the composite film can exhibit a combination of properties from both monomers. This allows for the fine-tuning of specific characteristics based on the desired application. The presence of VA units can introduce flexibility and enhance film transparency, while MA units can improve adhesion and compatibility with other materials [24,25].

Researchers have been reporting different properties of organic PP thin films, however, the reports on the effect of mixing two or more organic monomers for preparing composite polymer thin films are scanty, though only a few researchers reported the importance of bilayer or composite films but the deposition techniques they used are different from ours [6,11,17,23]. In this study, the elemental composition, surface morphology, and chemical bonding of the PPMA, PPVA, and PP(MA-VA) thin films deposited under dynamic low-pressure plasma were observed using energy dispersive x-ray, field emission scanning electron microscopy, and Fourier-transform infrared spectroscopy analysis, respectively. The optical properties of the composite films with different MA and VA ratios were analyzed using UV–vis spectroscopy to determine parameters such as absorbance, transmittance, reflectance, absorption coefficient, direct and indirect band gap, extinction coefficient, Urbach energy, refractive index, etc. This study presents a novel approach to fabricating composite thin films with improved surface morphology, tunable films thickness and enhanced films stability. The optical band gap of the composite films can be tuned by adjusting the monomer ratio. This means that the band-gap values of the films can be modified by varying the proportion of methyl acrylate monomer. This tunability is important as it allows tailoring the optical properties of the films for specific application requirements. These findings contribute to the field of materials science and provide potential opportunities for the development of advanced electronic and optoelectronic devices. The results of these investigations are correlated to evaluate the structural and optical improvement of composite thin films, which may be suitable in high-performance electronic and optoelectronic devices.

2. Materials and methods

2.1. The monomers

The PP composite thin films were prepared using two monomers, MA (>99.98%) and VA (>99.97%), which were obtained from BDH, Poole, England and Merck, Germany, respectively. The chemical structures and the general properties of the monomers are presented in Fig. 1 and Table 1, respectively.

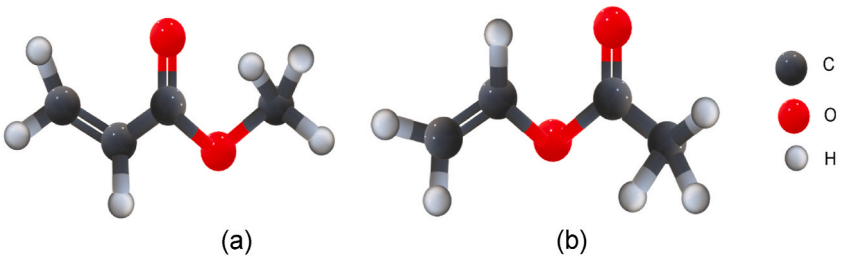

Fig. 1. The chemical structures of the (a) MA and (b) VA monomers.

Table 1
General properties of the MA and VA [26,27].

	Methyl acrylate (MA)	Vinyl acetate (VA)
IUPAC name	Methyl prop-2-enoate	Ethenyl acetate
Chemical formula	$CH_2CHCO_2CH_3$	$CH_3CO_2CHCH_2$
Appearance	Colorless liquid	Colorless liquid
Toxicity	Non-toxic	Less toxic
Boiling point	353 K	345.7 K
Molecular Weight	86.09 g/mol	86.09 g/mol
Density	950 kg/m^3	934 kg/m^3

2.2. Synthesis of the thin films

Before deposition, glass substrates (Sail brand, China, 25.4 × 76.2 × 1.2 mm^3) were cleaned in three steps so that a uniform, smooth, and perfect thin polymer plasma coating can be obtained. First, the substrates were soaked in detergent water for 15 min and washed with clean water. The cleaned substrates were again rinsed with acetone in an ultrasonic bath for another 15 min. Finally, those were rinsed again with de-ionized water and dried with hot air. The cleaned glass slides were preserved in a vacuum desiccator for deposition purposes. To deposit the composite thin film onto the pre-cleaned glass substrate, the monomer was allowed to enter a vacuum plasma chamber as shown in Fig. 2. Before that, the reactor chamber was slowly pumped down to 13.33 Pa using a rotary pump, and the two parallel plates were powered by an AC (50 Hz, 22 W) source to produce glow discharge plasma around the electrodes. A detailed description of the PP deposition technique is described in an earlier publication [28]. A fine injection valve was used to adjust the monomer flow rate to 20 cm^3/min. The working pressure during the deposition (60 min) was kept stable around 33.33 Pa. The films were deposited varying the amount of MA monomer as 100%, 75%, 50%, 25% and 0% in the mixture of MA and VA, and the composite films were termed respectively, as PPMA, PP(MA-VA) (3:1), PP(MA-VA) (1:1), PP(MA-VA) (1:3) and PPVA.

The thicknesses, *d*, of the as-deposited homo and composite thin films were measured by well-known multiple-beam interferometric technique [29] and calculated using Eq. (1).

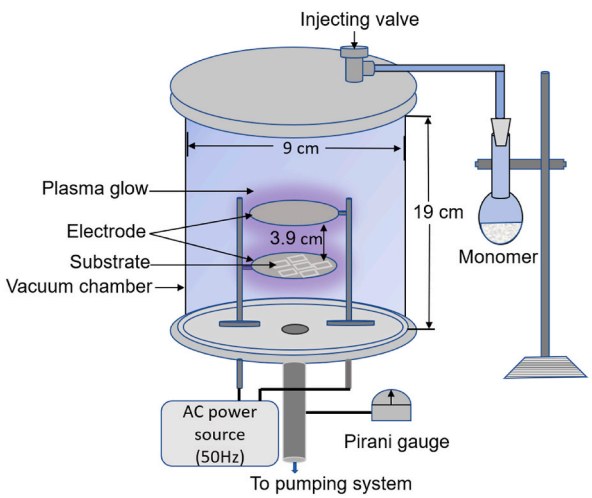

Fig. 2. Schematic diagram of the plasma polymerization set up in the laboratory.

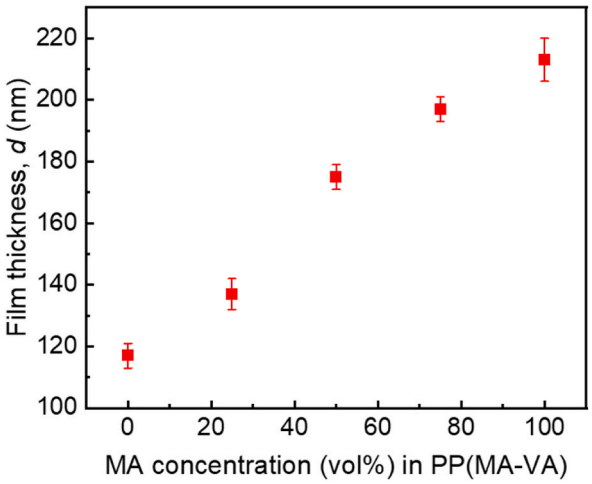

Fig. 3. The variation of thickness with the variation of MA concentration in the monomer.

Table 2
The mixing ratio of the monomer concentration as well as determined thickness and sample identification of the as-deposited composite thin films.

Mixing ratio of the monomer		Deposition time (min)	Thickness, d (nm)	Sample identity
Methyl acrylate (MA)	Vinyl acetate (VA)			
100%	0	60	213 ± 7	PPMA
75%	25%	60	197 ± 4	PP(MA-VA) (3:1)
50%	50%	60	175 ± 4	PP(MA-VA) (1:1)
25%	75%	60	137 ± 5	PP(MA-VA) (1:3)
0	100%	60	117 ± 4	PPVA

$$d = \frac{\lambda}{2}\frac{b}{a} \tag{1}$$

where, $\lambda = 589.3$ nm for sodium light source, b is the step height and a is the fringe spacing identified in the fringes. A recent publication has described in detail the thickness-measuring procedures using multiple-beam interferometric technique [30]. The variation of as-prepared films thickness with respect to MA concentration in the monomer mixture is illustrated in Fig. 3 and it is found that the thickness of the composite thin films decreases with decreasing MA concentration, which is presented in Table 2. As MA is a highly active monomer with a higher deposition rate compared to VA, the film thickness increase with the increase of MA monomer in the composite mixture.

2.3. Characterization techniques

The surface morphology and cross-sectional view of the as-deposited thin films were observed using FESEM (JEOL JSM 7600 F, USA) at an accelerating potential of 5 kV. The PPMA, PPVA and PP(MA-VA) thin films were coated with platinum to avoid charging effect during the measurement. EDX studies linked to the FESEM have also corroborated the compositional components of the films. The FTIR spectra of the samples were taken in the wavenumber range of 500–4000 cm^{-1} using a double-beam FTIR spectrometer (SIMADZU, FTIR-8400) with a resolution of 2 cm^{-1} to detect various types of bond vibration and to elucidate the chemical structure of the MA and VA monomers as well as PPMA, PPVA, and PP(MA-VA) thin films. The polymers are collected in powder form from the substrate by scrapping method. A dual-beam UV–Vis spectrophotometer (SHIMADZU UV-2600, Japan) coupled with an integrating sphere was used to measure the optical absorbance (A), transmittance (T) and reflectance (R) of the thin films in the wavelength range of 200–800 nm. The data were used to calculate the optical band gap energy as well as other vital optical parameters such as absorption coefficient (α), Urbach energy (E_U), extinction coefficient (k), steepness parameter (σ_s), and refractive index (μ), etc. A pre-cleaned glass substrate, similar to that onto which thin films were deposited, was used as a reference.

3. Results and discussion

3.1. Surface morphology

The surface morphology of the as-deposited PP homo and composite thin films as shown in Fig. 4(a_1-b_1), reveals that the surfaces of the homopolymer films are quite different compared to those of the composite films. Some agglomerate or mosaic structures or white

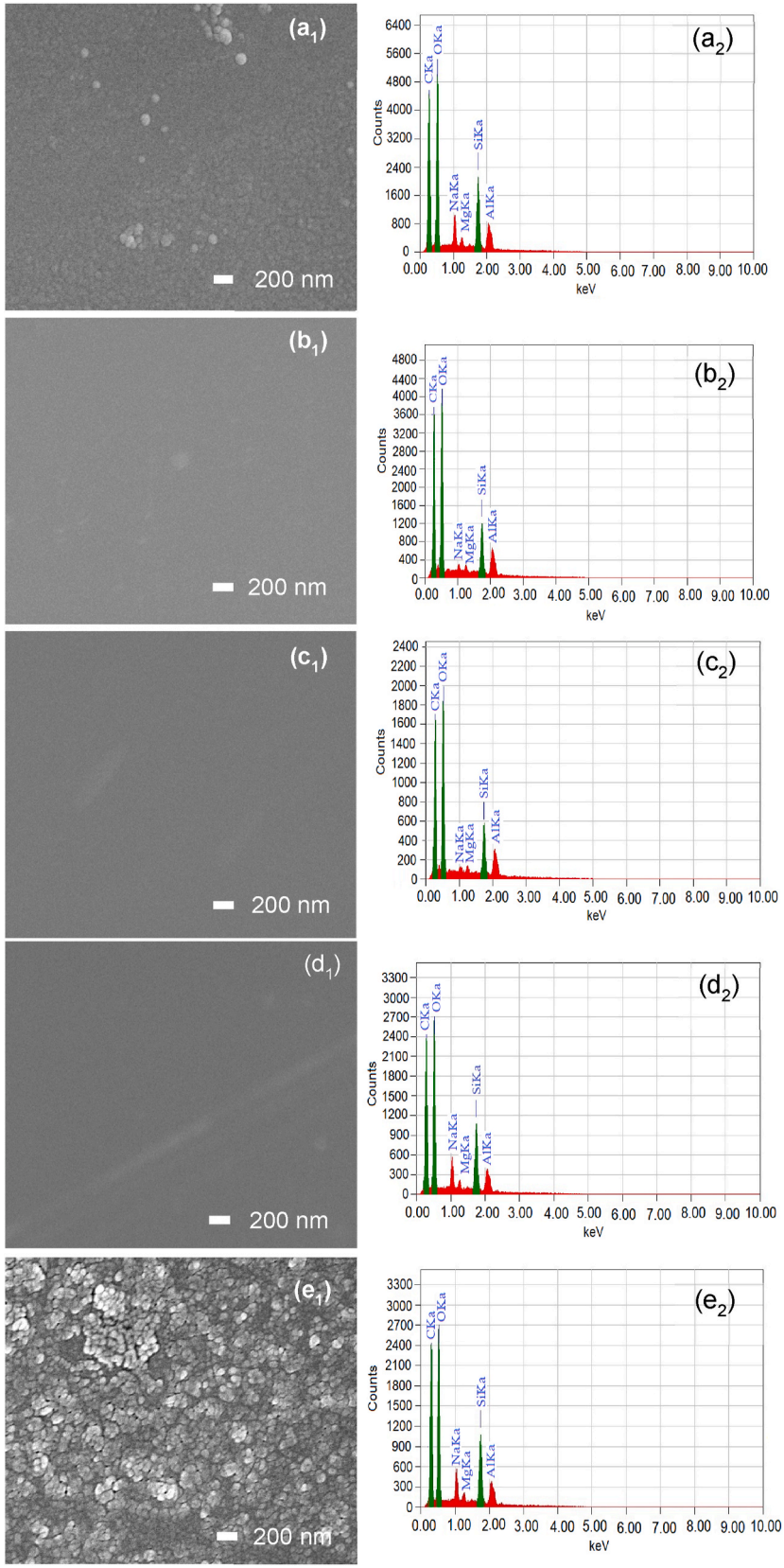

(caption on next page)

Fig. 4. FESEM images (a_1–e_1) and EDX spectra (a_2–e_2) of the *as*-deposited deposited (a_1, a_2) PPMA, (b_1, b_2) PP(MA-VA) (3:1), (c_1, c_2) PP(MA-VA) (1:1), (d_1, d_2) PP(MA-VA) (1:3), and (e_1,e_2) PPVA thin films with a magnification of 30 k.

spots are visible in both PPMA and PPVA homopolymer thin films, which may be caused by the aggregation of molecules or formation of cluster as a result of the interaction between the molecular chains [28,31]. Similar type of surface morphology was also observed in a previous study conducted by Nath and Bhuiyan [32] using the same procedure on PPMA thin film. The mosaic type structures are more prominent on the surface of PPVA film. This could be due to the individual chemical and physical properties of the VA monomer used to prepare the films. However, the composite thin films exhibit significantly better surface morphology with no mosaic type structure at the same magnification. In all cases, the films are pinhole-free, scratch-less, flawless and smooth because the composition of two monomers enhanced the high crosslinking properties among the plasma ions, radicals, or molecules through collisions with energetic electrons, which reduced the polymer chain and resulted in a better surface property of the composite films [33,34]. This type of smooth and pinhole-free surface was also observed in other studies using D-limonene and 3, 4-ethylenedioxythiophene where both the films were deposited by the plasma technique [5,30].

Cross-sectional images of the composite films shown in Fig. 5 confirm the formation of a homogeneous and smooth thin layer on the glass substrate and found that the thickness of PP(MA-VA) (3:1), PP(MA-VA) (1:1) and PP(MA-VA) (1:3) films were 139, 170 and 200 nm, respectively which was very near to the values of 137, 175 and 197 nm, respectively examined by the multiple-beam interferometric technique. This result ensures the accuracy and reliability of the thickness of the composite film.

3.2. Elemental analysis

The EDX analysis of the as-deposited homo and composite films has revealed the constituent elements of the films. The EDX spectra show that the atomic percentage of carbon varied for all the deposited films, which may be due to the removal of hydrogen atoms during the formation of plasma polymers. The MA and VA contain only carbon (C), hydrogen (H), and oxygen (O). But no hydrogen spectra were detected, because, due to the absence of K shell in the hydrogen atoms, the EDX method cannot detect any H atoms [35]. The PPMA and PPVA contain 26.09 and 28.03 at% of C, respectively whereas, for the composite films, the C percentage was increased to 34.44–37.20 at% which may be the cause of the higher crosslinking effect of MA and VA molecules. The higher carbon content in the composite film indicates a greater presence of carbon-based functional groups, which can contribute to improved film properties [36]. The smoother surface of the composite films also supports this phenomenon. Moreover, the O at% is greater in all deposited films compared to the calculated values of the monomer, which may be due to the bond formation among glass substrates and the monomer molecules during thin film deposition. Apart from these, the EDX data reveals the presence of some additional elements such as silica, sodium, magnesium and aluminum. These additional elements also may come from the glass substrate used for deposition [32]. In Fig. 4(a_2–b_2), the EDX spectra are presented, and Table 3 lists the atomic percentages of constitutive and other elements details for PPMA, PPVA and PP(MA-VA) films.

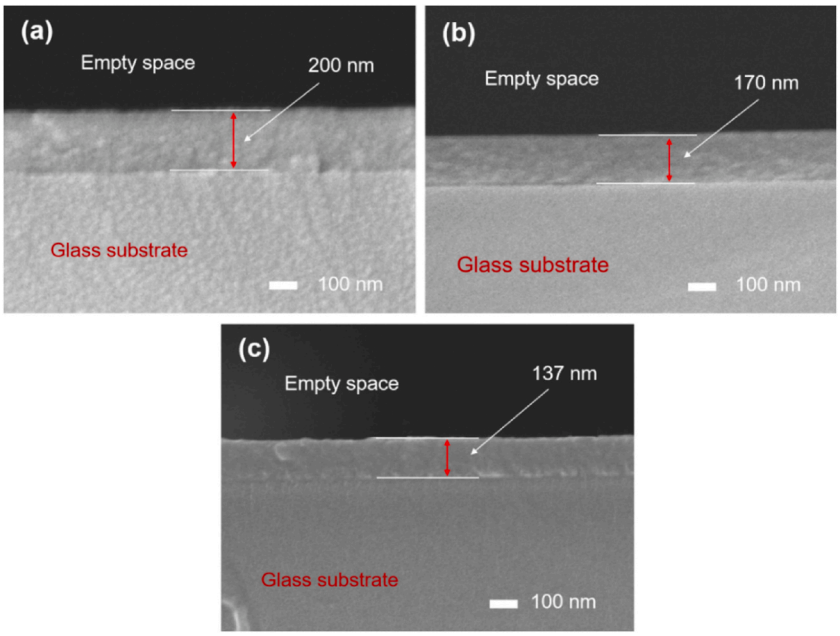

Fig. 5. FESEM (cross-sectional view) of the as-deposited (a) PP(MA-VA) (3:1), (b) PP(MA-VA) (1:1), (c) PP(MA-VA) (1:3) thin films.

Table 3
Atomic percentage (at%) of the elements in the PP homo polymer and composite polymer thin films.

Element detected	Elements in PP(MA-VA) composite thin films (at%)					Monomer (at%) (calculated from molecular formula)	
	PPMA	PP(MA-VA)			PPVA		
		3:1	1:1	1:3		MA	VA
C	28.03	37.20	36.22	34.44	26.09	55.80	55.80
O	38.51	38.40	40.10	38.26	35.03	37.17	37.17
H	–	–	–	–	–	7.02	7.02
Na	8.44	3.20	2.44	3.26	10.33	–	–
Mg	2.17	3.00	2.67	3.17	5.19	–	–
Si	17.02	12.00	12.89	15.65	18.35	–	–
Al	5.83	6.20	5.68	5.22	5.01	–	–
Total	100	100	100	100	100	100	100

3.3. FTIR analysis

The FTIR spectra of the homo and composite polymer films with various MA and VA mixing conditions have been taken at room temperature in the wavenumber range of 500–4000 cm^{-1} which are illustrated in Fig. 6. The identified bond assignments of different absorption peaks are documented in Table 4. In the FTIR spectra of both the monomer as well as of the homo and composite polymers a broad absorption band is appeared around 3438 − 3470 cm^{-1} due to −O H stretching, because of having chemical interaction between the carbonyl (C═O) groups and the H atoms, which helps to form hydrogen bonds and conjugated carbonyl with the methylene of MA and VA [37]. However, the intensity of this absorption peak in the PP films is not as strong as in the monomer spectra and broadness increases, which indicates that the PP films do not attach easily to the atmospheric low molecular weight molecules like H_2O and CO_2 [38]. In the FTIR spectra the absorption peaks at 2922 − 2970 cm^{-1} can be assigned to the stretching vibration of methyl group (−CH_3), while the absorption peaks appeared at 1375 − 1448 cm^{-1} are due to the bending vibration of C–H [39]. These peaks are important to recognize the compounds as organic compounds. The presence of a sharp absorption peak in the spectra of MA and VA at 1734 and 1741 cm^{-1} can be attributed to the strong vibration of the C═O groups present in the two individual monomer segments [16]. Whereas, this absorption band for PPMA, PPVA, and PP(MA-VA) composites shifted towards 1700 − 1709 cm^{-1} but become broad and weak, which confirms the structural change during the formation of all these thin films [39]. It is noticed that the intensity of the absorption peak for C═O group is higher for PPMA compared to PPVA, since the propagation rate of acrylate (CH_2═CH − COO −) is higher compared to that of VA monomer, which also has a significant effect on how fast the polymer is formed [19].

The sharp peaks of C═C stretching vibration in the monomers appeared at 1645 cm^{-1}, which become diffused and shifted between 1633 and 1645 cm^{-1} in the case of pp polymers. The asymmetric bending of –CH_3 corresponding to wavenumber 1436 − 1464 cm^{-1} is observed in all spectra. The shift in this absorption peaks towards the lower wavenumber (1379 − 1385 cm^{-1}) of all the deposited PP films spectra is due to –CH_2 bending vibrations which are caused for the loss of hydrogen atoms in –CH_3 depending on a variety of factors, including the chemical structure and molecular interactions. The absorption peaks in the 800 − 1282 cm^{-1} range are typically associated with C − O and C═C complex stretching vibrations [39–41]. The relative proportion of hydrophilic (C − O) and hydrophobic (C − H and C═C) groups in FTIR spectra reveal that the deposited PP films are more hydrophobic compared to the individual MA and VA monomers and from the deposited films the PP(MA-VA) films are less hydrophilic than PPMA and PPVA. The appearance of absorption band at 648–678 cm^{-1} in VA accompanying to C–H out-of-plane bending and shifting of this to a higher wavenumber is also a strong sign of conjugation in the chemical structure [18].

3.4. Optical properties

The UV–Vis absorption spectra in the wavelength range of 250–800 nm of the homopolymer and composite thin films deposited with varying monomer ratios at ambient temperature are illustrated in Fig. 7 (a). The A is maximum for the PPMA thin film, and as the content of MA in the composite films decreases the intensity of the absorbance peak also decreases which may be due to the decrease in the $\pi-\pi^*$ transition [42]. The wavelength corresponding to the maximum absorbance (λ_{max}) is observed to shift towards the higher wavelength (red shift). This shifting indicates an increase in conjugate bond length during the polymer formation and causes a change in the optical band gap of the obtained composite thin films [10,43]. This also suggests the alteration in the chemical composition of the film with different MA and VA ratios, which affects the absorption properties of the film. The λ_{max} and absorbance values corresponding to the different monomer ratios in the PP(MA-VA) thin films are summarized in Table 5.

The optical T (Fig. 7(b)) of the composite films rises with λ in the lower visible range (350–550 nm) and finally reaches almost a constant value of around 86 − 97% at higher wavelengths (550–800 nm). The composite films have higher transmittance in the lower wavelength range compared to PPMA and PPVA films may be due to their different crosslink density [44]. This difference in crosslinked density may be the cause of the varying transmittance properties of the deposited films. Despite this, all the films are highly transparent in the visible region.

The α was calculated from A and the path length that is the thickness of the films, d, using Eq. (2).

$$\alpha = \frac{2.303\,A}{d} \tag{2}$$

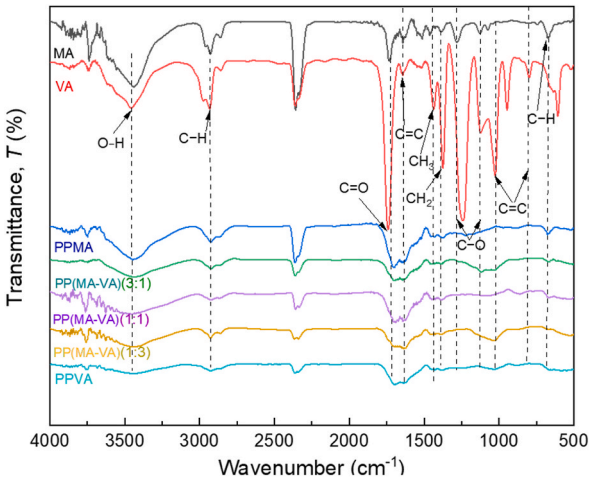

Fig. 6. The FTIR spectra of the MA and VA monomers, PPMA, PPVA homopolymer, and PP(MA-VA) composite thin films indicating different functional groups.

Table 4
Functional groups and the corresponding wavenumber in the MA and VA monomers, PPMA, PPVA and PP(MA-VA) thin films.

Assignment	MA	Wavenumber (cm^{-1})					VA	Band intensity
		PP(MA-VA)						
		PPMA	3:1	1:1	1:3	PPVA		
O − H stretching	3438	3443	3442	3470	3443	3444	3443	Broad peak
C − H_3 stretching	2961	–	–	–	–	–	2980	Merged
C − H_2 stretching	2938	2926	2928	2928	2922	2918	2938	Sharp
C − H stretching	2862	2860	2860	2860	2860	2860	2860	Merged
C = O stretching	1734	1709	1702	1700	1700	1705	1741	Broad peak
C═C stretching	1645	1636	1635	1634	1635	1633	1638	Very low
CH_3 bending	1464	1448	1448	1445	1448	1445	1436	Merged
CH_2 bending	1385	1380	1380	1380	1379	1379	1375	Low
C − O	1282,						1243,	Sharp peak
	1128	1167	1122	1269	1156	1200	1125	Merged
C═C bending	1024	1024	1031	1030	1027	1023	1025	low merged
				863	852	860	800	Low
C − H out of plane bending	676	674	681	678	660	685	648	Low

Here, $A = \log_{10}\left(\frac{I_0}{I}\right)$ with I_0 as the incident beam intensity and I being the transmitted beam intensity. From the variation of α with photon energy, $h\nu$, as shown in Fig. 8(a) it is noticed that the α changes with $h\nu$ following an exponential decay in the low-energy region, which is occurred due to the lack of long-range order in the films or the existence of defects [45].

The optical band gap, E_g, indicates the optical transitions of a substance, which is one of the most crucial optical properties associated with the electronic structure of a film. A direct band gap, $E_{g(d)}$ refers to a material where the electron transition between the valence and conduction bands is allowed in a single step, and the energy required for this transition is equal to the band gap. The indirect band gap, $E_{g(i)}$ is not allowed in a single step and requires the involvement of phonons (lattice vibrations) to conserve momentum.

The Tauc relation (Eq. (3)) is utilized to calculate the permissible optical band gaps of the thin film [46].

$$\alpha h\nu = C\,(h\nu - Eg)n \tag{3}$$

where, the index, n, indicates the nature of the optical transition, and the Tauc parameter, C, is a proportionality factor. The value of $n = 1/2$ and 2 indicates the allowed $E_{g(d)}$ and $E_{g(i)}$, respectively. Therefore, $E_{g(d)}$ and $E_{g(i)}$ are assessed respectively from the intercept of the linear part of the $(\alpha\, h\nu)^2$ versus $h\,\nu$ and $(\alpha\, h\nu)^{1/2}$ versus $h\,\nu$ curves, as shown in Fig. 8 (b) and 8(c), respectively.

The non-linear variation of α in PP(MA-VA) thin films indicates that two types of band gaps are possible in PP(MA-VA) composite films, which is also reported for several other plasma polymers [21,47,48]. The calculated values of $E_{g(d)}$ and $E_{g(i)}$ of the PPMA, PPVA, and PP(MA-VA) thin films are figured out in Table 5.

The $E_{g(d)}$ is observed to be different for all the composite films since some individual crosslinking may be established among the bulk of the two different monomers, which impacts the deposition process [40]. The values of $E_{g(d)}$ for PPMA and PPVA film are 2.77 eV and 2.72 eV, respectively and for the PP(MA-VA) composite films, it increases (3.00 − 3.15 eV) with increasing MA concentration in

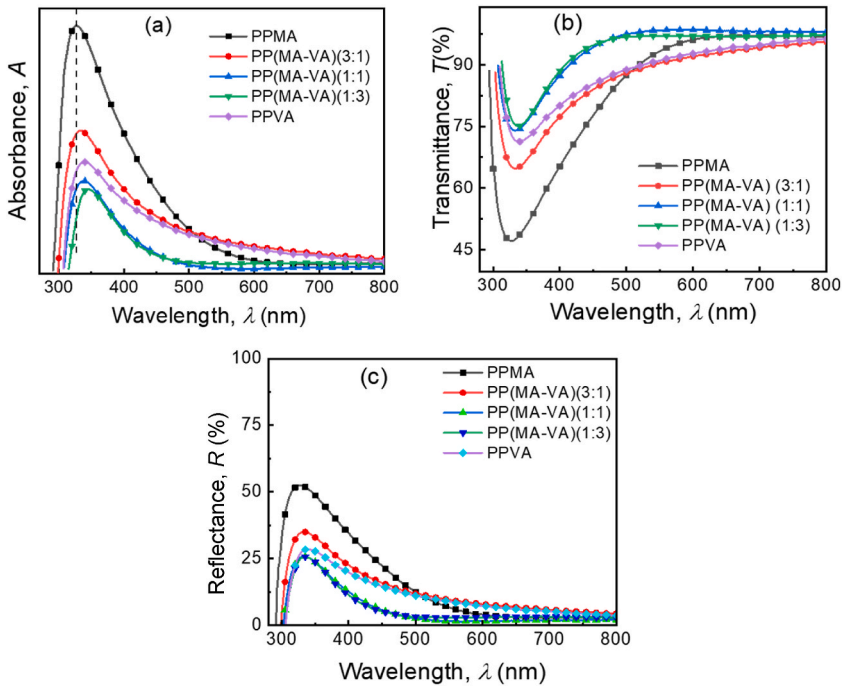

Fig. 7. Spectral distribution of (a) absorbance, (b) transmittance and (c) reflectance as a function of wavelength for different monomer ratios of MA and VA.

Table 5
Variation of Eg, λ_{max}, EU and σ s values of the PPMA, PPVA, and PP(MA-VA) thin films of different monomer ratios.

Sample ID	Thickness, d (nm)	λ_{max} (nm)	$E_{g(d)}$ (eV)	$E_{g(i)}$ (eV)	E_U (eV)	σ_s	$E_{e\text{-}p}$
PPMA	213 ± 7	326	2.77	1.84	0.42	0.10	6.67
PP(MA-VA) (3:1)	197 ± 4	332	3.15	2.35	0.33	0.12	5.55
PP(MA-VA) (1:1)	175 ± 4	336	3.12	2.26	0.46	0.09	7.40
PP(MA-VA) (1:3)	137 ± 5	345	3.00	1.74	0.90	0.05	13.3
PPVA	117 ± 4	340	2.72	1.70	0.96	0.04	16.60

the composite films. The red shift in absorbance spectra and the decrease in film thickness with the decrease of MA monomer suggest a fall in E_g values [49]. The $E_{g(i)}$ values of PPMA and PPVA are 1.84 eV and 1.70 eV, respectively and for the PP(MA-VA) composite films, the $E_{g(i)}$ values vary from 1.74 eV to 2.35 eV, depending on the concentration of MA in the composite films. For thin solar films, generally, wide band gap materials having $E_{g(d)}$ of the order of 2.0–4.0 eV permit devices to operate at much higher voltages and frequencies than conventional semiconductor materials [50]. The variation of $E_{g(d)}$ and $E_{g(i)}$ values with MA, and the tabulated values of E_g suggest an idea of tuning the optical band gap by varying the monomer ratios in composite films. The direct band gap of the PP (PA-VA) films is 3.00–3.15 eV, and it has good transparency in the visible region. So, it may be used in thin solar films and other optoelectronic applications.

The localized defect states in the optical band gap region are accountable for the creation of an absorption tail in the spectra, which is recognized as Urbach tail, and the associated energy is known as Urbach energy, E_U. It represents the defect states in the optical band gap region and is estimated for the plasma polymers. The Urbach empirical rule that describes the spectral dependence of α on $h\nu$ in the low photon energy region is given by Eq. (4) [51].

$$\alpha = \alpha_0 \, exp\left(\frac{E}{E_U}\right) \tag{4}$$

where, α_0 is a constant, and E is the energy of the incident photon. The inverse of the lnα versus $h\nu$ plots in Fig. 8(d) indicates the Urbach energy. It is observed that the values of E_U for PPMA and PPVA are 0.42 and 0.96 eV, respectively. However, the E_U values for the composites are observed to become higher (0.33 − 0.90 eV) for the lower amount of MA. This indicates that when MA is decreased in the composite films, it creates more localized states which form additional distribution defects within the forbidden energy band gap. Consequently, causes a shrinkage in the optical band gap and decreases the band gap energy [30,31].

The steepness parameter, σ_s is a measure of the rate of change α near the absorption edge and can provide valuable information about the electronic structure and optical properties of the films, which can be estimated by using Eq. (5) [52].

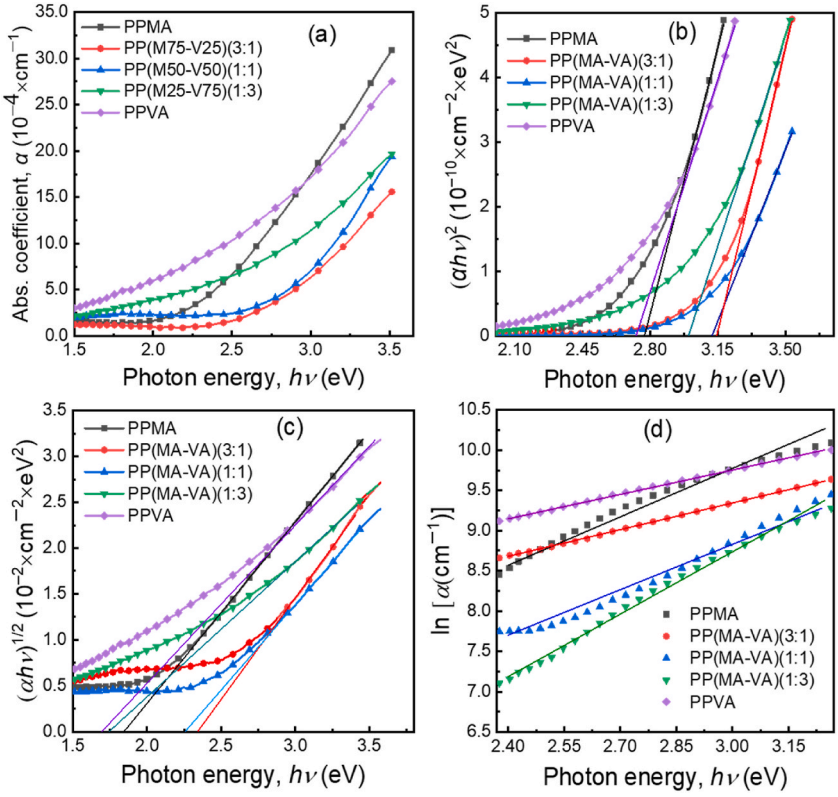

Fig. 8. Plots of (a) absorption coefficient, α, corresponding to photon energy and the corresponding graphs to obtain (b) direct band gap, $E_{g(d)}$, (c) indirect band gap $E_{g(i)}$, and (d) lnα versus $h\nu$ plots for the as-deposited PP homo and composite thin films.

$$\sigma = \frac{k_B T}{E_U} \tag{5}$$

Here T is the absolute temperature and k_B is the Boltzmann constant. The σ_s values are calculated by taking $T = 298$ K. The observed lower values of σ_s (0.10 − 0.26), indicate a smaller density of states near the absorption edge and a lower rate of electron-phonon scattering, resulting in a narrower absorption edge [53].

The σ_s values of as-deposited films are shown to have a relationship with the strength of the electron-phonon ($E_{e\text{-}p}$) interaction as indicated by Eq. (6) [54]-

$$E_{e-p} = \frac{2}{3\sigma_s} \tag{6}$$

The values of $E_{e\text{-}p}$ are tabulated in Table 5 and are found to range from 2.56 to 6.67, showing an inverse relationship with the σ_s values. This information provides insight into the electronic structure and optical properties of the PP(MA-VA) thin films and can be useful for various applications such as optoelectronics and solar cell technology.

Another crucial optical parameter allied with the absorption of a material is k. The optical constant of the material k obtained using α with the assistance of Eq. (7), which describes the attenuation of light in a medium.

$$k = \frac{\alpha\lambda}{4\pi} \tag{7}$$

The value of k is dependent on the wavelength of light and the concentration of absorbing species in the medium. The higher k indicates the greater the amount of light absorbed by the material. Fig. 9 (a) depicts that the value of k decreases with the increase of λ, which indicates a possible reduction in electron transfer across the mobility gap with λ.

The μ is the measure of the reduction of speed of light inside a material and is used to measure the light propagation through a material. The higher the value μ the greater the deviation of light from a straight path, and the slower the speed of light in the material. The values of μ are evaluated using Fresnel's Eq. (8) [55,56], and the variation with λ is presented in Fig. 9 (b).

$$\mu = \left(\frac{1+R}{1-R}\right) + \sqrt{\frac{4R}{(1-R)^2} - k^2} \tag{8}$$

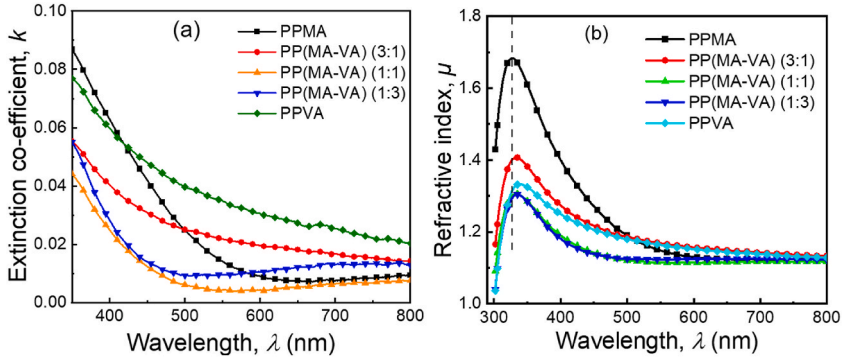

Fig. 9. The variation of (a) extinction coefficient and (b) refractive index with λ for the as-deposited homopolymers and composite polymers of various monomer ratios.

It is pointed out that the μ value is maximum at a lower wavelength of 330 nm then drops suddenly in the wavelength region at 340 – 550 nm and becomes almost stable (~1.14) indicating higher transmittance properties in the UV region for all the PP(MA-VA) composite films. Nevertheless, the maxima in the μ values lifted from 320 nm to 340 nm with the variation of monomer mixture ratios, which confirms the increase in photon-electron interactions inside the films.

4. Conclusions

PPMA, PPVA, and PP(MA-VA) composite thin films have been deposited successfully onto glass substrates by the dynamic low pressure plasma polymerization technique. The thickness of the composite films varies from 137 to 197 nm with a higher proportion of MA. Notably, the composite films exhibit improved surface morphology, characterized by a higher amount of carbon content, thereby enhancing their structural properties. The chemical structures of homo polymer and composite polymer thins films are transformed during the polymerization, which is confirmed by the FTIR analysis. The disappearance of the absorption peak in the fingerprint region indicates exceedingly crosslinking properties of the PP thin films. Moreover, The composite film exhibits enhanced transmission performance in the visible region of the electromagnetic spectrum. The optical parameters of the composite film are found to be varied with varying MA and VA monomer ratios, where the homopolymer films are independent of each other. It is observed that the values of $E_{g(d)}$ and $E_{g(i)}$ of the composite films vary from 3.00 to 3.15 eV and 1.74–2.35 eV, respectively, with the enhancement of the MA monomer. Those values are quite different from PPMA ($E_{g(d)} = 2.77$ eV, $E_{g(i)} = 1.84$ eV) and PPVA ($E_{g(d)} = 2.72$ eV, $E_{g(i)} = 1.70$ eV) homopolymer thin films. The decrease of E_U values from 0.90 to 0.33 eV with the increase in MA in the composite films suggest that the optical band gap is reduced owing to the appearance of localized states inside the forbidden energy band gap region. The change in μ specifies the rise of interactions between the photons and electrons of the composite films with the increase of MA. The probability of electron transfer across the mobility gap rises with photon energy, which is confirmed by analyzing the obtained extinction co-efficients. Overall, the PP(MA-VA) composites exhibit superior and more stable properties compared to PPMA and PPVA homopolymer thin films. The thickness, optical band gap, and other optical parameters can be tailored to meet specific requirements by adjusting the ratio of MA and VA in the composite films. Decisively, the PP(MA-VA) thin composite films are found to be chemically, physically, and optically stable and the films may be a potential candidate for photovoltaic and organo-electronic applications. The investigated characteristics of PP(MA-VA) composite thin films in this study have shown a significant dependency on the varying ratios of MA and VA. This observation suggests the potential utilization of composite film as an adaptable substitute for organo-semiconducting materials in natural systems.

Author contribution statement

Md. Saddam Sheikh: Conceived and designed the experiments; Performed the experiments; Analyzed and interpreted the data; Wrote the paper.

Md. Juel Sarder: Performed the experiments; Analyzed and interpreted the data.

A. H. Bhuiyan: Analyzed and interpreted the data; Wrote the paper.

Mohammad Jellur Rahman: Analyzed and interpreted the data; Contributed reagents, materials, analysis tools or data; Wrote the paper.

Data availability statement

Data will be made available on request.

Declaration of competing interest

The authors declare that they have no known competing financial interests or personal relationships that could have appeared to influence the work reported in this paper.

Acknowledgments

The authors are grateful to the Committee for Advanced Studies and Research (CASR), Bangladesh University of Engineering and Technology (BUET), for providing financial support for this work. They also acknowledge the Department of Chemistry, BUET and Bangladesh Council of Scientific and Industrial Research (BCSIR) for providing necessary laboratory supports.

References

[1] K. Wu, Y. Yu, Z. Hou, X. Guan, H. Zhao, S. Liu, T. Zhang, A humidity sensor based on ionic liquid modified metal organic frameworks for low humidity detection, Sensor. Actuator. B Chem. 355 (2022), 131136, https://doi.org/10.1016/j.snb.2021.131136.
[2] R. Morent, N. De Geyter, J. Verschuren, K. De Clerck, P. Kiekens, C. Leys, Non-thermal plasma treatment of textiles, Surf. Coating. Technol. 202 (2008) 3427–3449, https://doi.org/10.1016/j.surfcoat.2007.12.027.
[3] N.A. Ibrahim, B.M. Eid, M.S. Abdel-Aziz, Effect of plasma superficial treatments on antibacterial functionalization and coloration of cellulosic fabrics, Appl. Surf. Sci. 392 (2017) 1126–1133, https://doi.org/10.1016/j.apsusc.2016.09.141.
[4] P.A. Wilbon, F. Chu, C. Tang, Progress in renewable polymers from natural terpenes, terpenoids, and rosin, macromol, Rapid Commun. 34 (2013) 8–37, https://doi.org/10.1002/marc.201200513.
[5] D. Gerchman, B. Bones, M.B. Pereira, A.S. Takimi, Thin film deposition by plasma polymerization using d-limonene as a renewable precursor, Prog. Org. Coating 129 (2019) 133–139, https://doi.org/10.1016/j.porgcoat.2019.01.018.
[6] S.P. Russell, D.H. Weinkauf, Vapor sorption in plasma polymerized vinyl acetate and methyl methacrylate thin films, Polymer (Guildf) 42 (2001) 2827–2836, https://doi.org/10.1016/S0032-3861(00)00677-7.
[7] A.A. Kehail, V. Boominathan, K. Fodor, V. Chalivendra, T. Ferreira, C.J. Brigham, Vi vo and in vitro degradation studies for poly(3-hydroxybutyrate-co-3-hydroxyhexanoate) biopolymer, J. Polym. Environ. 25 (2017) 296–307. https://doi:10.1007/s10924-016-0808-1.
[8] W.T. Ting, K.S. Chen, M.J. Wang, Dense and anti-corrosion thin films prepared by plasma polymerization of hexamethyldisilazane for applications in metallic implants, Surf. Coating. Technol. 410 (2021), 126932, https://doi.org/10.1016/j.surfcoat.2021.126932.
[9] H. Akther, A.H. Bhuiyan, H. Kabir, R. Nasrin, M.M. Rahman, Understanding the enhancement of the optical and electronic attributes of iodine-doped vacuum deposited tetramethylaniline (PPTMA) thin film coatings, J. Alloys Compd. 874 (2021), 159989, https://doi.org/10.1016/j.jallcom.2021.159989.
[10] N.S. Wadatkar, S.A. Waghuley, Synthesis and complex optical characterization of polythiophene/poly (vinyl acetate) composite thin films for optoelectronic device applications, Indian J. Pure Appl. Phys. 60 (2022) 430–436. http://nopr.niscpr.res.in/handle/123456789/59707.
[11] Z. Khattari, M. Maghrabi, T. McNally, S. Abdul Jawad, Impedance study of polymethyl methacrylate composites/multi-walled carbon nanotubes (PMMA/MWCNTs), Phys. B Condens. Matter 407 (2012) 759–764, https://doi.org/10.1016/j.physb.2011.12.019.
[12] F.H. Abd-El Kader, W.H. Osman, R.S. Hafez, DC conduction mechanism and dielectric properties of Poly (methyl methacrylate)/Poly (vinyl acetate) blends doped and undoped with malachite green, Phys. B Condens. Matter 408 (2013) 140–150, https://doi.org/10.1016/j.physb.2012.09.027.
[13] P. Tallury, N. Alimohammadi, S. Kalachandra, Poly(ethylene-co-vinyl acetate) copolymer matrix for delivery of chlorhexidine and acyclovir drugs for use in the oral environment: effect of drug combination, copolymer composition and coating on the drug release rate, Dent. Mater. 23 (2007) 404–409, https://doi.org/10.1016/j.dental.2006.02.011.
[14] H. Yasuda, Q. Yu, Creation of polymerizable species in plasma polymerization, Plasma Chem. Plasma Process. 24 (2004) 325–351, https://doi.org/10.1023/B:PCPP.0000013204.17559.72.
[15] S. Schiller, J. Hu, A.T.A. Jenkins, R.B. Timmons, F.S. Sanchez-Estrada, W. Knoll, R. Förch, Chemical structure and properties of plasma-polymerized maleic anhydride films, Chem. Mater. 14 (2002) 235–242, https://doi.org/10.1021/cm011139r.
[16] M.S. Islam, J.H. Yeum, A.K. Das, Synthesis of poly(vinyl acetate-methyl methacrylate) copolymer microspheres using suspension polymerization, J. Colloid Interface Sci. 368 (2012) 400–405, https://doi.org/10.1016/j.jcis.2011.11.002.
[17] H. Eisazadeh, Copolymerization of aniline and vinyl acetate by using various surfactants in aqueous media, J. Appl. Polym. Sci. 13 (2007) 229–233, https://doi.org/10.1002/vnl.20133.
[18] M.M. Kamal, A.H. Bhuiyan, Optical characterization of plasma-polymerized pyrrole-N,N,3,5-tetramethylaniline bilayer thin films, J. Appl. Polym. Sci. 121 (2011) 2361–2368, https://doi.org/10.1002/app.33176.
[19] J. Li, X. Pan, N. Li, J. Zhu, X. Zhu, Photoinduced controlled radical polymerization of methyl acrylate and vinyl acetate by xanthate, Polym. Chem. 9 (2018) 2897–2904, https://doi.org/10.1039/C8PY00050F.
[20] E.Y. Jung, C.S. Park, H.J. Jang, G.T. Bae, B.J. Shin, H.S. Tae, Synthesis and characterization of poly(pyrrole-co-aniline) copolymer using atmospheric pressure plasma polymerization, Mol. Cryst. Liq. Cryst. 733 (2022) 103–113, https://doi.org/10.1080/15421406.2021.1972205.
[21] A.M. Abdelghany, M.S. Meikhail, N. Asker, Synthesis and structural-biological correlation of PVC\PVAc polymer blends, J. Mater. Res. Technol. 8 (2019) 3908–3916, https://doi.org/10.1016/j.jmrt.2019.06.053.
[22] C. Ennawaoui, A. Hajjaji, C. Samuel, E. Sabani, A. Rjafallah, I. Najihi, E.M. Laadissi, E.M. Loualid, M. Rguiti, A. El Ballouti, A. Azim, Piezoelectric and electromechanical characteristics of porous poly(Ethylene-co-vinyl acetate) copolymer films for smart sensors and mechanical energy harvesting applications, Appl. Syst. Innov. 4 (2021) 57, https://doi.org/10.3390/asi4030057.
[23] O.G. Zamyshlyayeva, B.N. Ionychev, M.A. Baten'kin, N.A. Kopylova, A.V. Markin, S.D. Zaitsev, Y.D. Semchikov, Properties of methacrylic acid–methyl acrylate, Russ. J. Appl. Chem. 91 (2018) 1332–1337, https://doi.org/10.1134/S1070427218080116.
[24] S.M. Alqahtani, R.S. Al Khulaifi, M. Alassaf, W.S. Saeed, I. Bedja, A. Aldarwesh, A. Aljubailah, A. Semlali, T. Aouak, Preparation and characterization of poly (vinyl acetate-co-2-hydroxyethyl methacrylate) and in vitro application as contact lens for acyclovir delivery, Int. J. Mol. Sci. 24 (2023) 5483, https://doi.org/10.3390/ijms24065483.
[25] N. Deka, A. Bera, D. De, P. Roy, Methyl methacrylate-based copolymers: recent developments in the areas of transparent and stretchable active matrices, ACS Omega 7 (2022) 36929–36944, https://doi.org/10.1021/acsomega.2c04564.
[26] T. Liu, Q. Liu, Y. Liu, H. Yao, Z. Zhang, X. Wang, J. Shen, Fabrication of methyl acrylate modified silica aerogel for capture of Cu2+ from aqueous solutions, J. Sol. Gel Sci. Technol. 98 (2021) 389–400, https://doi.org/10.1007/s10971-021-05499-w.
[27] M. Abdollahi, P. Bigdeli, Reverse iodine transfer radical copolymerization of vinyl acetate and vinyl benzoate: a kinetic study, Polym. Bull. 75 (2018) 1823–1841, https://doi.org/10.1007/s00289-017-2130-z.
[28] R. Nasrin, M.J. Rahman, A.T.M.K. Jamil, K.S. Hossain, A.H. Bhuiyan, Thickness dependent structural and surface properties of plasma polymerized N-benzylaniline thin films, Appl. Phys. Mater. Sci. Process 127 (2021) 1–12, https://doi.org/10.1007/s00339-021-04326-x.
[29] S. Tolansky, Mehrfachreflex-interferometrie an oberflächen und schichten, Phys. J. 4 (11–12) (1948) 472–480, https://doi.org/10.1002/phbl.19480041105.
[30] J. Sarder, M. Hasan, A.H. Bhuiyan, M. Jellur, Thickness dependence of structural and optical behavior of plasma polymerized 3 , 4-ethylenedioxythiophene thin films, Opt. Mater. 134 (2022), 113170, https://doi.org/10.1016/j.optmat.2022.113170.

[31] A.S. Hassanien, I.M. El Radaf, A.A. Akl, Physical and optical studies of the novel non-crystalline CuxGe20-xSe40Te40 bulk glasses and thin films, J. Alloys Compd. 849 (2020), 156718, https://doi.org/10.1016/j.jallcom.2020.156718.
[32] S.D. Nath, A.H. Bhuiyan, Surface morphology and optical properties of thin films of plasma polymerized methyl acrylate, Opt. Mater. 136 (2023), 113474, https://doi.org/10.1016/j.optmat.2023.113474.
[33] N. Banu, A.H. Bhuiyan, K.S. Hossain, Characterization of structural and optical properties of plasma polymerized diethanolamine thin films, Adv. Polym. Technol. 37 (2018) 3084–3094, https://doi.org/10.1002/adv.22079.
[34] H.J. Jang, E.Y. Jung, T. Parsons, H. Tae, C. Park, A review of plasma synthesis methods for polymer films and nanoparticles under atmospheric pressure conditions, Polymers 13 (2021) 2267, https://doi.org/10.3390/polym13142267.
[35] H. Akther, M.M. Rahman, A.H. Bhuiyan, H. Kabir, S.A. Al Zumahi, J.A. Syed, R. Nasrin, Carrier transport mechanisms of iodine-doped plasma polymerised N, N, 3, 5 tetramethylaniline thin films, Mater. Today Commun. 31 (2022), 103377, https://doi.org/10.1016/j.mtcomm.2022.103377.
[36] S. Kumar, K. Jayanarayanan, M. Balachandran, High-performance thermoplastic polyaryletherketone/carbon fiber composites: comparison of plasma, carbon nanotubes/graphene nano-anchoring, surface oxidation techniques for enhanced interface adhesion and properties, Compos. B Eng. 253 (2023), 110560, https://doi.org/10.1016/j.compositesb.2023.110560.
[37] A. Ramírez-Hernández, C. Aguilar-Flores, A. Aparicio-Saguilán, Fingerprint analysis of ftir spectra of polymers containing vinyl acetate, Dyna 86 (2019) 198–205, https://doi.org/10.15446/dyna.v86n209.77513.
[38] D.U. Park, J.H. Ryu, N.K. Han, W.H. Park, Y.G. Jeong, Thermal analysis on the stabilization behavior of ternary copolymers based on acrylonitrile, methyl acrylate and itaconic acid, Fibers Polym. 19 (2018) 2439–2448, https://doi.org/10.1007/s12221-018-8782-y.
[39] E. Yu, L. Zhang, Y. Zhang, Z. Liu, T. Wang, X. Liu, W. Eli, Synthesis of gemini-like methyl acrylate-acrylic acid-methyl acrylate triblock copolymers surfactants by RAFT polymerization in solution and investigation of their behavior at the air-water interface, J. Surfactants Deterg. 18 (2015) 729–738, https://doi.org/10.1007/s11743-015-1708-4.
[40] R.T. Conley, Infrared Spectroscopy, Allyn and Bacon Inc Boston, 1972.
[41] C.N. Banwell, E.M. McCash, Fundamentals of Molecular Spectroscopy, fourth ed., McGraw-Hill, London, 1994.
[42] O. Bayram, O. Simsek, A study on the optical, chemical and dielectric properties of PPCIN thin films derived from essential oil compounds using RF plasma polymerisation technique, Vacuum 156 (2018) 198–204, https://doi.org/10.1016/j.vacuum.2018.07.032.
[43] Z. Xu, L. Kong, Y. Wang, B. Wang, J. Zhao, Tuning band gap, color switching, optical contrast, and redox stability in solution-processable BDT-based electrochromic materials, Org. Electron. 54 (2018) 94–103, https://doi.org/10.1016/j.orgel.2017.12.014.
[44] D.C. Guerin, D.D. Hinshelwood, S. Monolache, F.S. Denes, V.A. Shamamian, Plasma polymerization of thin films: correlations between plasma chemistry and thin film character, Langmuir 18 (2002) 4118–4123, https://doi.org/10.1021/la011566j.
[45] A. Dolgonos, T.O. Mason, K.R. Poeppelmeier, Direct optical band gap measurement in polycrystalline semiconductors: a critical look at the Tauc method, J. Solid State Chem. 240 (2016) 43–48, https://doi.org/10.1016/j.jssc.2016.05.010.
[46] J. Tauc, A. Menth, D.L. Wood, Optical and magnetic investigations of the localized states in semiconducting glasses, Phys. Rev. Lett. 25 (11) (1970) 749–752, https://doi.org/10.1103/PhysRevLett.25.749.
[47] A.M.E. Sayed, A.M. Abdelghany, A. Abou Elfadl, Structural, optical, mechanical and antibacterial properties of MgO/poly(vinyl acetate)/poly(vinyl chloride) Nanocomposites, Braz. J. Phys. 52 (2022) 1–12, https://doi.org/10.1007/s13538-022-01156-x.
[48] R.A. Elsad, K.A. Mahmoud, Y.S. Rammah, A.S. Abouhaswa, Fabrication, structural, optical, and dielectric properties of PVC-PbO nanocomposites, as well as their gamma-ray shielding capability, Radiat. Phys. Chem. 189 (2021), 109753, https://doi.org/10.1016/j.radphyschem.2021.109753.
[49] N.S. Wadatkar, S.A. Waghuley, Characterizing the electro-optical properties of polyaniline/poly(vinyl acetate) composite films as-synthesized through chemical route, Results Surf. Interf. 4 (2021), 100016, https://doi.org/10.1016/j.rsurfi.2021.100016.
[50] P.N. Kalu, C. Augustine, A.N. Nwachukwu, R.A. Chikwenze, S.O. Amadi, B.J. Robert, P.E. Okpani, T.O. Daniel, C.N. Ukwu, E.P. Obot, C.O. Dike, R.O. Okoro, Comparative analysis of the effect of annealing temperature on the structural and optical properties of chemically deposited CeO2/ZnO and CeO2/NiO core-shell thin films for photovoltaic and optoelectronic applications, Chalcogenide Lett. 18 (2021) 649–665. https://chalcogen.ro/649_KaluPN.pdf.
[51] A.S. Hassanien, I. Sharma, P. Sharma, Inference of Sn addition on optical properties of the novel thermally evaporated thin a-Ge15Te50S35-xSnx films and some physical properties of their glasses, Mater. Chem. Phys. 293 (2023), 126887, https://doi.org/10.1016/j.matchemphys.2022.126887.
[52] S. Solaymani, S. Ţălu, N. Beryani Nezafat, L. Dejam, A. Shafiekhani, A. Ghaderi, A. Zelati, Optical properties and surface dynamics analyses of homojunction and hetrojunction Q/ITO/ZnO/NZO and Q/ITO/ZnO/NiO thin films, Results Phys. 29 (2021), 104679, https://doi.org/10.1016/j.rinp.2021.104679.
[53] F.O. Efe, B. Olofinjana, O. Fasakin, M.A. Eleruja, E.O.B. Ajayi, Compositional, structural, morphological, optical and electrical property evolutions in MOCVD Cu-Zn-S thin films prepared at different temperatures using a single solid source precursor, J. Electron. Mater. 48 (2019) 8000–8013, https://doi.org/10.1007/s11664-019-07636-2.
[54] S. Ebrahimi, B. Yarmand, N. Naderi, High-performance UV-B detectors based on MnxZn1-xS thin films modified by bandgap engineering, Sensor Actuator Phys. 303 (2020), 111832, https://doi.org/10.1016/j.sna.2020.111832.
[55] M. Isik, N.M. Gasanly, Linear and nonlinear optical properties of Bi12GeO20 single crystal for optoelectronic applications, Mater. Sci. Semicond. Process. 153 (2023), 107170, https://doi.org/10.1016/j.mssp.2022.107170.
[56] J.I. Pankove, Optical Processes in Semiconductors, Prentice-Hall, Englewood Cliffs, New Jersey, 1971.